Acta Biomaterialia 8 (2012) 2730–2736

Contents lists available at SciVerse ScienceDirect

Acta Biomaterialia

journal homepage: www.elsevier.com/locate/actabiomat

In vivo dynamics of the internal fibrous structure in smooth adhesive pads of insects

Jan-Henning Dirks [a,*], MingHe Li [b], Alexandre Kabla [c], Walter Federle [a]

[a] Department of Zoology, University of Cambridge, Cambridge CB2 3EJ, UK
[b] Department of Control Science, Tongji University, Shanghai, People's Republic of China
[c] Department of Engineering, University of Cambridge, Cambridge CB2 1PZ, UK

ARTICLE INFO

Article history:
Received 4 January 2012
Received in revised form 20 March 2012
Accepted 3 April 2012
Available online 9 April 2012

Keywords:
Biomechanics
Insect adhesion
Insect cuticle
Biomaterials
Poisson's ratio

ABSTRACT

Many insects with smooth adhesive pads can rapidly enlarge their contact area by centripetal pulls on the legs, allowing them to cope with sudden mechanical perturbations such as gusts of wind or raindrops. The short time scale of this reaction excludes any neuromuscular control; it is thus more likely to be caused by mechanical properties of the pad's specialized cuticle. This soft cuticle contains numerous branched fibrils oriented almost perpendicularly to the surface. Assuming a fixed volume of the water-filled cuticle, we hypothesized that pulls could decrease the fibril angle, thereby helping the contact area to expand laterally and longitudinally. Three-dimensional fluorescence microscopy on the cuticle of smooth stick insect pads confirmed that pulls significantly reduced the fibril angle. However, the fibril angle variation appeared insufficient to explain the observed increase in contact area. Direct strain measurements in the contact zone demonstrated that pulls not only expand the cuticle laterally, but also add new contact area at the pad's outer edge.

1. Introduction

Many insects possess fluid-mediated foot pads that can adhere securely to almost all known surfaces [1,2]. Whilst the adhesive pads of several insect groups such as flies and beetles are densely covered with flexible setae, the smooth pads found in other insects such as ants, stick insects and cockroaches are "pillow-like" soft structures. Although distinct in morphology, both designs provide good adhesion to surfaces with unpredictable roughness by maximizing the contact area between the pad and the surface. In smooth adhesive pads a two-phase adhesive secretion helps to fill gaps between small surface asperities and allows the insects to combine capillary adhesion with resistance against sliding [3].

Besides the presence of an adhesive emulsion, an additional remarkable adaptation of the smooth arolia is the highly specialized adhesive cuticle. It is characterized by fibrils which are oriented almost perpendicularly to the surface [4–8]. Scanning electron microscopy (SEM) of freeze fractures and transission electron microscopy (TEM) of the arolium of stick insects (*Carausius morosus*) showed that these cuticular rods originate from the endocuticular layer and are 44–74 μm long with an average diameter of 1.65 μm. Towards the surface, the thick rods branch into finer fibrils [7]. This specialized type of cuticle has evolved several times independently in arthropods, but its detailed function is still unclear [9]. The branched fibril structure probably helps the pads to conform to surface roughness at different length scales [10]. Moreover, it has been proposed that the fibrous structure is responsible for the pads' frictional anisotropy, i.e. the higher friction of pads in the pulling direction, which allows animals to increase adhesion by opposing their feet, thereby achieving shallower force vectors [11,12]. It has been found that this direction dependence is largely explained by the variation in adhesive contact area [1]. However, it is still unclear what role the fibrillar ultrastructure plays in this dynamic reaction.

A dynamic control of adhesive contact area has been demonstrated for ants that can actively and passively change the size of their contact area [13]. When the legs are pulled towards the body, ant adhesive pads in partial contact with a surface can rapidly unfold. Due to the "chain-like" morphology of the segmented insect tarsus, a distal adhesive pad can transmit significant forces only in the pulling direction, and both pushing forces and lateral forces are likely small. The passive, purely mechanical nature of the ants' unfolding reaction is confirmed by the finding that it can occur extremely fast, sometimes within less than a millisecond [14]. This passive increase of adhesive contact area allows insects to react quickly to mechanical perturbations such as wind or raindrops [13,15]. Neuronally controlled reflexes in insects typically take much longer (>5 ms in the locust leg [16]; 10–15 ms for *Blatta orientalis* and *Periplaneta americana* [17]). This delay clearly excludes a neuromuscular control of the contact area within this time frame [13,16].

* Corresponding author. Present address: Department of Mechanical and Manufacturing Engineering, Trinity College Dublin, Dublin 2, Ireland. Tel.: +353 1 896 1464.
E-mail address: jan-henning.dirks@web.de (J.-H. Dirks).

1742-7061/$ - see front matter © 2012 Acta Materialia Inc. Published by Elsevier Ltd. All rights reserved.
http://dx.doi.org/10.1016/j.actbio.2012.04.008

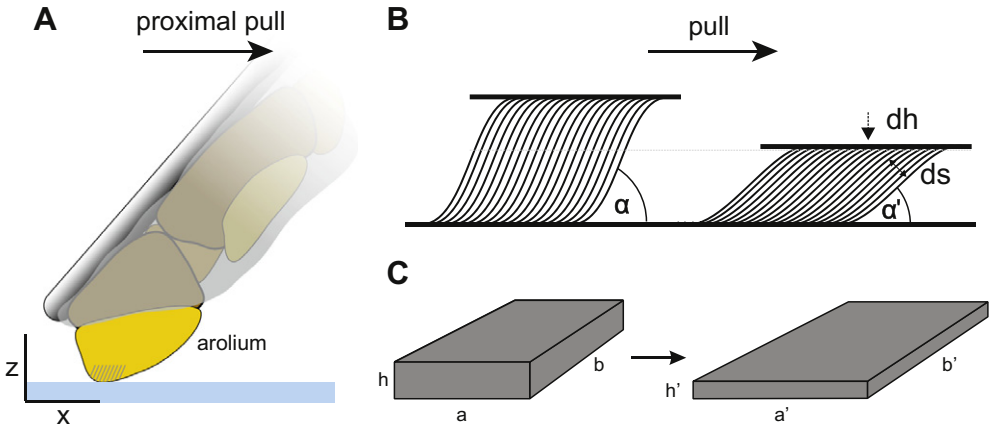

Fig. 1. Hypothetical model for the passive contact area increase of smooth pads. (A) Schematic drawing indicating the orientation of the cuticle fibrils in a fixed adhesive pad and the orientation of the axes used in this study. The lateral (transverse) y-axis is orientated perpendicular to the image plane. (B) A pulling movement of the pad on the surface may reduce the angle α of the cuticular fibres. Assuming a constant length of the fibrils, reducing the fibril angle will reduce the structure's height (h). If the structure's height decreases, the average spacing between the fibres ds (measured within the x–z-plane) will be reduced too. This "compression" might increase the bending stiffness of the adhesive pad. (C) If the volume of the fibrous cuticle is constant ($a \times b \times h$), decreasing its height to h' should enlarge the contact area by a factor of h/h'.

It is unlikely that such useful mechanical "preflexes" are confined to ants, and preliminary findings indeed indicate that a similar preflex reaction occurs in stick insects (*C. morosus*), where the arolium cannot be unfolded, in contrast to the situation in ants and bees [14]. Variation of the direction of the shear movement showed that the passive variation of contact area is direction dependent. As in ants, contact area increased for pulls and decreased for pushes [14].

If muscular control cannot explain the increase in contact area, what is the mechanism underlying these passive reactions? For the smooth pads of ants the passive unfolding of the pad is caused by the complex mechanical arrangement of the arolium [13]. However, no such morphological adaptation is present in the smooth pads of other insect species such as stick insects or cockroaches. Could the specialized cuticle of the pads itself play a role in the increase of contact area?

If shearing of the cuticle is linked to a change of the fibril orientation, a proximal pull (towards the body) should reduce the fibril angle and decrease the thickness of the adhesive cuticle. Assuming that the cuticle is a cuboid with constant volume (height × width × length), any change of fibril orientation should be correlated with a change of contact area, as the pad cuticle is expected to expand along the proximal–distal and the lateral axis when the thickness decreases. Conversely, a distal pushing movement (away from the body) may lead to an increased fibril angle, resulting in a contraction of the adhesive contact area and easier detachment (see Fig. 1).

In this study we test this hypothesis by using fluorescence and interference reflection microscopy to quantify *in vivo* the effect of proximal pulls on the fibril orientation and to measure the strain within the adhesive contact zone.

2. Materials and methods

2.1. Study animals

Adult female Indian stick insects (*C. morosus*) were taken from a laboratory colony in which insects were kept at 24 °C and fed with water and food *ad libitum*.

Making use of their natural stick-like mimesis posture with their legs in line with the body, the stick insects were slid into a glass Pasteur pipette with their front legs protruding. The tarsus of one leg was fixed to a rigid soldering wire attached to the pipette. The last tarsal segments and the non-adhesive dorsal side of the arolium were carefully embedded in fast-hardening dental cement (Protemp, ESPE) to prevent any active movements of the adhesive organ (see Fig. 1A).

2.2. Visualization of the fibril structure

The arolia of the fixed legs were brought into contact perpendicularly with a smooth glass coverslip ("normal" position). The insect was then carefully pulled over 50 µm in the proximal direction ("pull") using a micromanipulator (speed ~10 µm s^{-1}) mounted on the microscope stage. This small amplitude ensured that the adhesive pad remained in static contact with the substrate at all times, as any sliding movement with a resulting shift of the fibril pattern would have interfered with the automated fibril angle measurements.

The fibrous cuticle of the adhesive pad shows a characteristic blue autofluorescence under UV illumination. This suggests that it contains resilin (although more rigorous tests are required for confirmation), a protein providing high resistance to mechanical fatigue frequently found in regularly deforming cuticle [18,19]. Images were recorded using a mercury short-arc lamp (HBO 103 W/2, Osram) at an excitation wavelength of 365 nm and emission wavelengths of >425 nm. At this illumination the adhesive fluid within the contact zone did not fluoresce and thus did not interfere with the measurements.

A Leica DRM HC microscope equipped with a motorized stage (LSTEP, Märzhäuser) and a triggered camera (10 bit monochrome CCD QICam, INTAS) were used to capture image stacks at 100× magnification and a frame rate of 1 Hz (500 ms exposure time + 500 ms movement of the stage). These stacks consisted of 100 consecutive images focusing "into" the pad's cuticle (starting slightly outside the pad), and 100 images captured whilst focusing "out", with a z-distance between consecutive frames of 0.192 µm. For the analysis, we selected 50 consecutive frames from the inwards movement and the 50 corresponding frames from the outwards movement for the automated tracking, starting at ~4 µm focal depth. By comparing the "in" and "out" patterns, we checked the stacks for pad movements during the capturing process. Throughout the paper, we refer to the optical axis of the microscope (i.e. the axis perpendicular to the glass substrate) as the z-axis; the projection of the leg onto the surface (i.e. the direction

of the pushing/pulling movement) is called the x-axis and the transverse direction (orthogonal to x and z) is the y-axis (see Fig. 1).

Measurements of the contact area of the same pads were taken before and after the shear movement at 5× magnification using reflected light.

2.3. Reconstruction of the fibril structure

The human eye is very good at pattern recognition and pattern completion, even at relatively low signal-to-noise ratios [20,21]. While the small individual fibrils were not clearly visible on single images, the movement of the pattern was apparent in animated image stacks (see Supplementary videos 1 and 2 in Supplementary materials).

To eliminate any observer bias, all identification characteristics were removed from the image stacks and the data were analysed in random order. To reduce noise and increase the visibility of the fibrils, each frame was two-dimensionally fast Fourier transform bandpass filtered (90 nm–4.5 μm). Fibril angles were manually digitized from sagittal views in the middle of the pad using the ImageJ "volume viewer" plug-in [22] (the sagittal view corresponds to the x–z-plane in Fig. 1).

Using a different, automated image analysis method, we verified the fibril angle results obtained by digitization of sagittal views (see Supplementary videos 1 and 2). The fibril structure's displacement vectors from one image of the z-stack to the next were tracked using an optical flow algorithm [23], developed using the CImg library. As the depth (z-position) of the imaging plane was moved through the cuticle, the local rate of displacement with depth provided a measure of the fibril angle.

Data for fibril angles and contact area were tested for normal distribution using the Kolmogorov–Smirnov method, and paired t-tests were used to test for significant differences between the "normal" and the "pulled" group. If not stated otherwise, all values are given as means ± standard error (SE).

2.4. Direct strain measurements in the contact zone

To analyse the detailed mechanism of contact area increase, we studied the adhesive contact zone of stick insect arolia during pushing and pulling movements using interference reflection microscopy (at 100× magnification and monochromatic illumination of 546 nm). Stick insects were mounted as before, but on a micromanipulator outside the microscope stage, and the arolium of one foot was brought into contact with a glass coverslip mounted on a holder on the microscope stage. Three pairs of short (50 μm displacement) pulls and pushes were performed by moving the microscope stage, with a velocity of 100 μm s^{-1} and a 2 s pause after each movement.

Images of different regions of the contact zone were recorded at 2 Hz. To avoid blur during the pad movement, we analyzed the first or second frame after the pulls/pushes. The characteristic pattern of folds in the contact zone allowed us to quantify the strain both along the x- and the y-axis (i.e. proximal–distal and lateral) caused by the pushing–pulling movements (see Fig. 1A). We define strain for our situation as:

$$\epsilon = \frac{l_{pull} - l_{push}}{l_{push}}, \quad (1)$$

where l_{pull} and l_{push} are the distances between two characteristic points in the contact zone after a pull or push, respectively.

3. Results

3.1. Effect of pulling on the fibril angle

The UV fluorescence image stacks of *C. morosus* adhesive pads clearly revealed the three-dimensional, fibrous structure of the procuticle (see Fig. 2B and C).

The mean angle measured from reconstructed sagittal views of the fibril structure for the normal pad position was 71.26 ± 1.3° ($n = 10$). After the pulling movement the mean angle was significantly reduced to 61.44 ± 1.3° ($n = 10$, $t_9 = 7.43$, $P < 0.001$, see Fig. 3A).

The angles measured using the automated tracking set-up were consistent with the angles digitized from reconstructed sagittal views. A direct comparison between manual digitization and automated tracking showed perfect consistency (65.5° vs. 63.2°, see Supplementary video 2). However, although the automated tracking method provided reliable measurements for intermediate fibril angles, it could not reliably resolve smaller angles after proximal pulls. Thus the manual digitization of reconstructed sagittal views proved to be the better option.

3.2. Effect of pulling on the adhesive contact area

The contact areas of the adhesive pad were significantly higher after the pulling movement (paired t-test, $t = -11.40$, $P < 0.001$) with a mean of 60,144 μm^2 for the "normal" and a mean of 72,504 μm^2 for the "sheared" condition (see Fig. 3B). Thus, the pull increased the contact area on average by 20.80 ± 1.72% ($n = 10$).

After the pull, the proximal–distal "length" of the contact area (measured along the proximal–distal "middle line" of the contact area) was largely unchanged (paired t-test, $t_9 = -0.253$, $P > 0.05$), whereas the lateral (transverse) "width" significantly increased (paired t-test, $t_9 = 12.43$, $P < 0.001$). Therefore, the aspect ratio of the contact area (i.e. width/length) significantly increased from 2.70 ± 0.06 to 3.15 ± 0.06 (paired t-test, $t_9 = -4.37$, $P < 0.001$, see Fig. 4). These results show that the increase in contact area was mainly the result of the increased pad width while pad length remained largely constant.

The correlation between contact area size and fibril angle was measured by calculating the change in contact area per degree change in fibril angle for each pair of measurements. All ratios were negative and significantly different from zero (mean incline −1798 ± 499 μm^2 deg^{-1}, one-sample t-test, $t_9 = -3.6$, $P < 0.001$).

3.3. Strain in the contact zone

Direct measurements in the adhesive contact zone of stick insects using IRM confirmed the presence of strains (as defined by Eq. (1)), ranging from −4.0% to 8.7%. Strain was positive both in the proximal–distal and in the lateral directions (one-sample t-tests significant both for proximal–distal: $t_{39} = 2.92$, $P < 0.01$, and lateral: $t_{39} = 4.22$, $P < 0.001$; Fig. 5). However, the relative magnitude of the two in-plane strain components was different depending on the region on the pad. While proximal–distal and lateral strains were not significantly different from each other near the lateral (left and right) edges of the pad ($t_{23} = 1.62$, $P > 0.1$), the transverse strain dominated significantly in the middle of the contact zone ($t_{14} = 3.03$, $P < 0.01$, Fig. 5).

From the overall mean strains of 0.92% (proximal–distal) and 1.87% (transverse), it can be estimated that cuticle expansion during the pull should increase the adhesive contact area by 2.8%. For the pad studied in this experiment, contact area increased from 102,445 ± 1756 μm^2 (push) to 107,919 ± 1591 μm^2 (pull), i.e. by

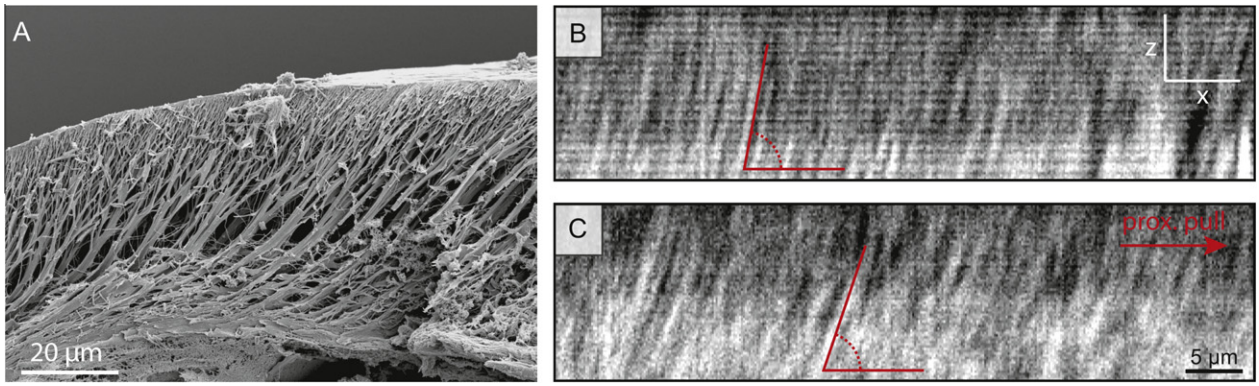

Fig. 2. (A) SEM image of a freeze fractured *C. morosus* arolium showing the branching fibrils within the outer cuticle layer. (B) *In vivo* fibril structure reconstructed from UV fluorescence image stacks of an adhesive pad in "normal" contact (*C. morosus*, contact area at top). (C) After a proximal pull the angle of the fibres to the cuticle surface decreased.

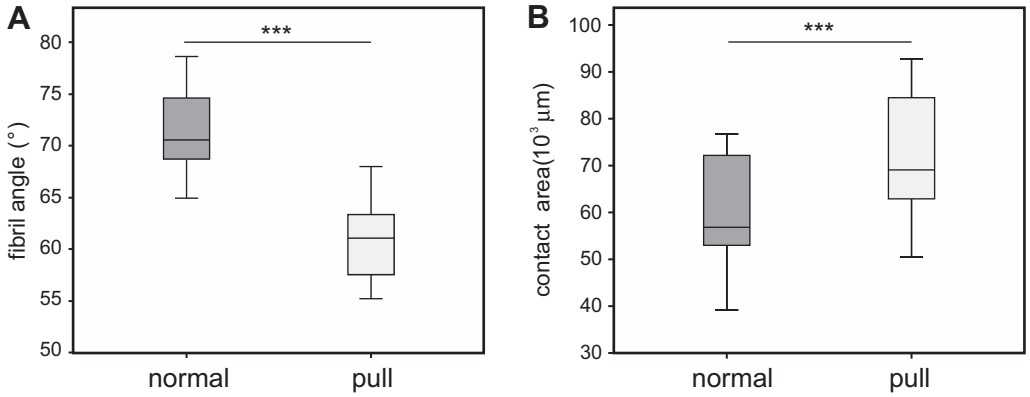

Fig. 3. (A) Fibril angles of one adhesive pad (*C. morosus*) before and after a proximal pull of 50 µm. The two groups are significantly different (paired *t*-test, $t_9 = 7.43$, $P < 0.001$). (B) After the pull the contact areas of the adhesive pad were significantly larger (paired *t*-test, $t_9 = -11.40$, $P < 0.001$).

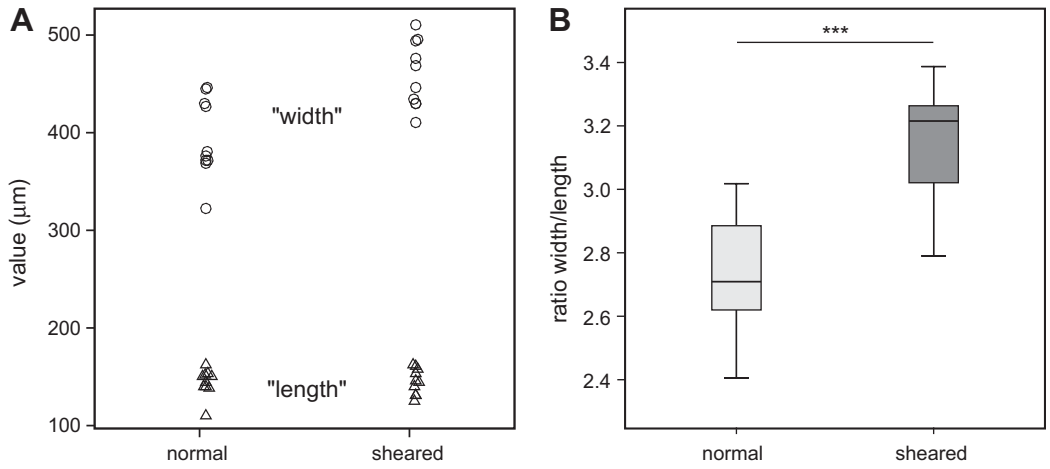

Fig. 4. Change in contact area proportions of *C. morosus* after a proximal pull of ~50 µm. (A) Whilst the proximal–distal "length" of the contact zone did not significantly increase after a pull, the lateral "width" did (for details see text). (B) After the pull the aspect ratio (width/length) of the contact area increased significantly.

5.3%. Thus, cuticle expansion only partly explains the observed increase in contact area.

At the same time, the IRM recordings showed that during pulls, new areas of adhesive cuticle came into contact at the edge of the pad. As we could only analyse image pairs where the pad edge was visible both after the pull and the push, our data do not allow a detailed assessment on which sides of the pad contact area was mainly gained (or lost). However, successful image pairs from the distal, lateral edges of the pad contact zone (see Fig. 5) show that the "new" cuticle zone added during the pull was as wide as 10.3 µm (measured perpendicularly to the pad edge; $n = 22$, median = 1.8 µm, range 0.2–10.3 µm).

Assuming that a cuticle zone of 1.8 µm width is added around the whole perimeter of the pad (length measured as 1350 µm),

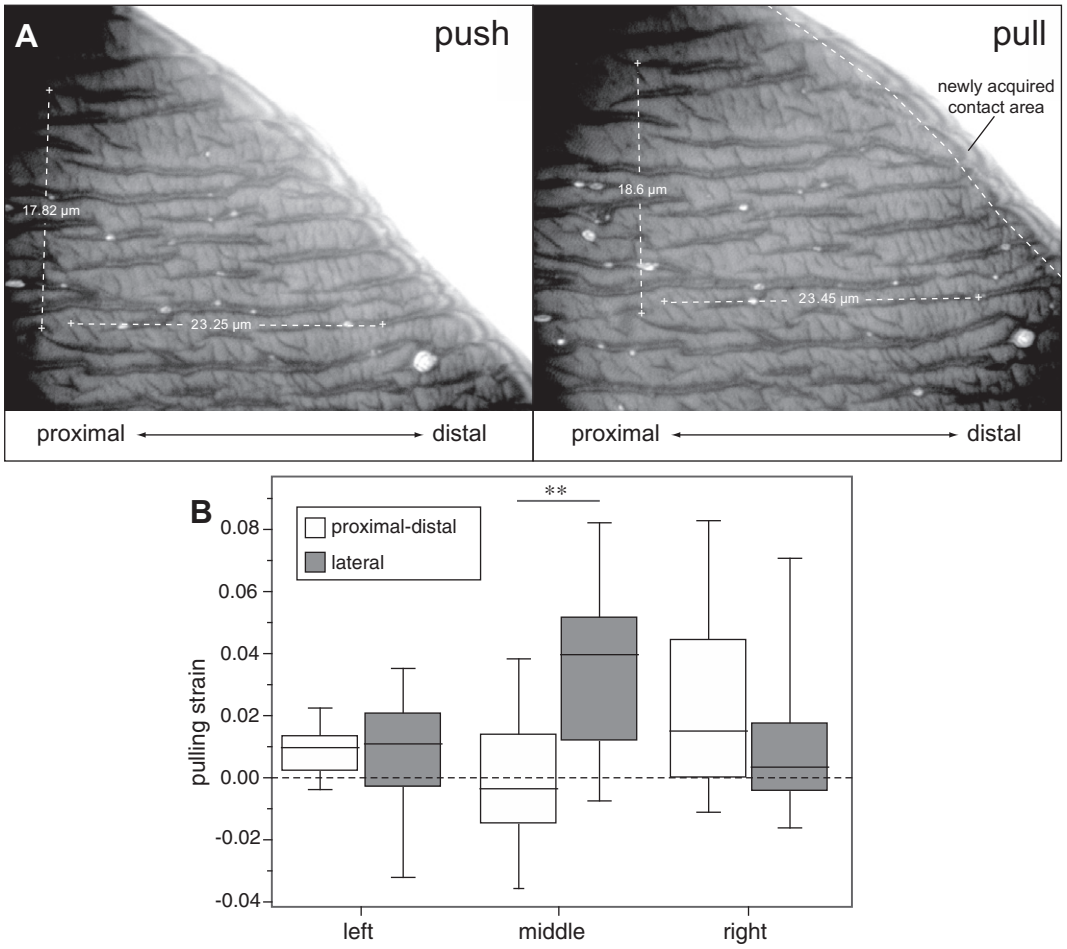

Fig. 5. Strain measurements in the adhesive contact zone of *C. morosus*. (A) Interference reflection microscopy images of corresponding area of the contact zone after a push (left) and a pull (right). Lines mark length measurements between corresponding landmarks on the pad to calculate proximal–distal and lateral strain. (B) Summary of proximal–distal and lateral strain measurements at different positions of the pad (left, middle and right region of the contact area). See text for the definition of pulling strain.

the contact area would grow by 2430 µm^2, i.e. by 2.4%. This value is in good agreement with the above estimate of 2.8%; the observed contact area increase of 5.3% therefore represents a combination of cuticular expansion (~54%) and addition of new contact area (~46%).

3.4. Regular microstructure in the outer arolium cuticle

When testing various combinations of surface properties to increase the visibility of the fibril pattern using interference reflection microscopy, we observed a regular "fingerprint"-like pattern on the arolia of *C. morosus* (see Fig. 6). The pattern consisted of a succession of bright and dark sinusoidal lines oriented transversely, i.e. perpendicular to the distal–proximal axis of the adhesive pad. The mean periodicity of the pattern along the proximal–distal axis was 414.4 ± 33 nm (n = 14).

The visibility of this pattern appeared to depend on the refractive index of the substrates. The pattern was visible on polyimide (PI-2611)-coated coverslips (n_0 = 1.9) and very clear on mica substrates ($n_0 \approx 1.59$), but showed only weak contrast on glass

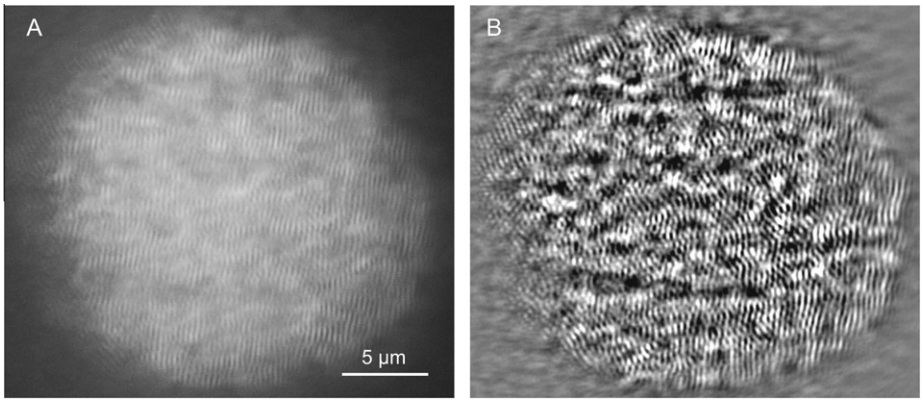

Fig. 6. (A) Interference reflection microscopy image of *C. morosus* arolium in contact with a mica surface (illuminating numerical aperture: 0.27, λ = 546 nm, brightness and contrast enhanced). (B) Fourier filtering of the image reveals a regular, fingerprint-like micropattern with a proximal–distal periodicity of 414.4 ± 33 nm (mean ± SE, n = 14). The proximal part of the arolium is on the right side of the images.

coverslips (n_0 = 1.52). The pattern was present throughout the entire contact area, and it was only visible in the outer zone of the cuticle, up to a focal depth of ~2 μm. Thus, this pattern did not interfere with our fibril angle measurements. The depth of the "fingerprint" pattern suggests that it is the result of a regular, directional arrangement of the fine cuticular fibrils in the outer "branching" zone of the arolium cuticle [7]. Higher-resolution electron microscopy imaging of this zone is required to test this hypothesis.

4. Discussion

Our study shows that *in vivo* measurements and 3-D reconstruction of the fibrils are possible with standard UV fluorescence microscopy. The fibril angles measured using the *in vivo* technique described here ranged between 55.19° and 78.62°. These results are in good agreement with 2-D SEM images of freeze-fractures of fixed adhesive organs (see Fig. 2A and Refs. [7,11]). As the weak UV autofluorescence of the cuticle required relatively long exposure times (500 ms), our recordings were limited to pads in completely static contact and therefore to small pulling forces. Although insect adhesive pads can generate some static friction [3,24,25], sliding is only absent for very small shear forces. As the friction of insect pads strongly increases with sliding velocity [24] shear forces can be more than 10 times larger than this "remaining" friction for faster pulls [3,25]. The fibril angle variation is probably a function of the applied force (acting against spring-like elements tending to return the fibres to their original position). Thus, it is likely that significantly smaller fibril angles will occur for the stronger pulling forces that insects experience under natural conditions. However, studying the fibril angles under such conditions will require new methods for statically applying large shear forces to the pad's cuticle.

A possible source of error in our fibril angle measurements are image distortions resulting from out-of-focus fluorescence. More advanced microscopy techniques such as confocal microscopy would probably improve the accuracy of the measurements. A better image quality would also facilitate the use of automated image-processing algorithms for fibril tracking, which are preferable in terms of speed. Computer-based image deconvolution can effectively reduce noise and increase the image quality of image stacks. However, computation times of 6–8 h for a single image stack currently restrict the practical use of this method.

4.1. Larger contact areas coincide with smaller fibril angles

Our results show that larger contact areas resulting from pulls coincided with smaller fibril angles. Even very weak pulls significantly increased the contact area and decreased the fibril angle. This finding confirms the validity of our hypothesis that shearing movements result in changes of the fibril orientation. Can the measured variation explain the observed change in contact area?

A simplified model can be used to estimate the effect of the fibrils on the contact area. If the length L of the fibrils is constant, and the cuticle height h is coupled with the fibril angle α ($0° < \alpha < 90°$), the height can be described by:

$$h = \sin\alpha \cdot L. \tag{2}$$

Assuming that the volume of the cuticle is constant ($A{\cdot}h = A'{\cdot}h'$), where A' and h' denote the contact area and height after a pull, respectively, the new contact area A' should depend on the change of the fibril angle (from α to α') as:

$$A' = A \cdot \frac{\sin\alpha}{\sin\alpha'}. \tag{3}$$

So far, no direct experimental support exists for the assumption of constant cuticular volume. However, the assumption is plausible because soft cuticle is a completely water-filled material that does not contain air [26], and water is effectively incompressible at physiological pressures. Thus, a volume change of the cuticle requires fluid flow into or out of this region of the cuticle, which may be slow as it has to pass perpendicularly through the outer membrane of the epidermal cells or laterally through adjacent, relatively thin and dense areas of cuticle. Particularly during rapid pad deformations such as those caused by sudden perturbations, the amount of fluid flow is probably negligible.

Eq. (3) shows that the observed change of α from 71.26° to 61.44° predicts an increase in contact area of 7.8%, which is smaller than the observed change of about 20%. This suggests that not only the fibre angle is responsible for the change in adhesive contact area.

One possibility is that a pull could slightly rotate the pad, thereby bringing new cuticle area into surface contact on its proximal side. While such a "rolling" movement would have a neutral effect on contact area for a spherical pad, the contact area could increase for other pad shapes such as asymmetrical "bean-like" pads, which have a smaller radius of curvature on the distal than on the proximal side. In this situation, even small changes of the pad's orientation could result in overproportional changes in contact area. A "rotation" model could also explain the observed change of the adhesive contact area's shape.

However, the results of our strain measurements in the adhesive contact zone speak against a simple "rotation" model. Firstly, we found that new contact area is also added at the distal margin of the contact zone. Secondly, the observed contact area increase occurred not only by the addition of new contact area at the pad edge but also by expansion of the adhesive cuticle.

Therefore, a third, related mechanism may apply, whereby both pad rotation and reduction of the fibril angle increase the hydrostatic pressure in the cuticle, tending to expand the contact area in all directions.

This prediction in turn contrasts with our finding that pulls significantly increased the "width" of the contact area but left the proximal–distal "length" virtually unchanged. The dominance of lateral over proximal–distal expansion was also evident from our strain measurements within the contact area. It therefore appears that despite a tendency to expand in all directions, the adhesive cuticle responds to pulls by elongating only slightly along the pull but strongly in the lateral direction. This behaviour may be based on the cuticle's ultrastructure. Lateral expansion may involve a lateral "fanning out" of the rods. While perfectly perpendicular rods should fan out equally well in the proximal–distal and the lateral directions, proximal–distal fanning may become constrained for smaller rod (fibril) angles so that lateral expansion should dominate. Moreover, the folding pattern in the adhesive contact zone (see Fig. 5A) might also play a role. As these folds run mainly along the proximal–distal axis, the cuticle and epicuticle may be more extensible in the lateral direction.

4.2. A proximal pull leads to a lateral expansion of the contact area

Our results show that the pad cuticle responds to a proximal–distal pull with a lateral expansion. This unusual behaviour suggests that smooth pad cuticle is a material with a negative Poisson's ratio. For a material, the Poisson's ratio is the negative of the ratio of lateral to axial strain under uniaxial extension or compression. Negative Poisson's ratios have been observed for some anisotropic crystals and materials comprised of fibrous networks [27–29].

The dynamic control of adhesive contact area investigated here for stick insects is analogous to the passive increase of adhesive

contact area in ants [13]. As in ants, a passive, purely mechanical "preflex" reaction may allow insects to respond instantly to perturbations tending to detach them from the substrate. Besides the advantage of a rapid contact area increase for unexpected mechanical perturbations, a change of the fibril angle could also assist a controlled peeling movement of the proximal rim of the contact zone. The stress distribution at the peeling edge is determined by the bending stiffness of the cuticle [30]. Reducing the fibril angle by a pull may result in a smaller proximal–distal distance between the single fibres, likely increasing the bending stiffness of the adhesive pad's cuticle. This would prevent peeling and thereby increase adhesive forces. Conversely, pushing movements may produce more perpendicularly orientated fibrils, making the cuticle more easily deformable and peelable and allowing easy detachment during locomotion.

While almost all previous attempts to produce biomimetic adhesives have focused on the gecko's fibrillar adhesive system, the potential of smooth pads as a source of inspiration is still untapped. Fibrous auxetic (negative Poisson ratio) structures might provide a new mechanism for adhesives to achieve rapid attachment and detachment via shear forces [12]. Application of this principle in synthetic adhesive pads may help the development of controllable adhesives and climbing robots.

Acknowledgements

This study was financially supported by fellowships of the German National Academic Foundation, the Irish Research Council for Science, Engineering and Technology (to J.-H.D.), the Biotechnology and Biological Sciences Research Council (BB/E004156/1 to W.F.) and a scholarship from Tongyi University (to M.L.). The SEM image in Fig. 2A was taken by Christofer Clemente.

Appendix A. Figures with essential colour discrimination

Certain figures in this article, particularly Figures 1 and 2, are difficult to interpret in black and white. The full colour images can be found in the on-line version, at http://dx.doi.org/10.1016/j.actbio.2012.04.008.

Appendix B. Supplementary data

Supplementary data associated with this article can be found, in the online version, at http://dx.doi.org/10.1016/j.actbio.2012.04.008.

References

[1] Bullock JMR, Drechsler P, Federle W. Comparison of smooth and hairy attachment pads in insects: friction, adhesion and mechanisms for direction-dependence. J Exp Biol 2008;211:3333–43.
[2] Dirks JH, Federle W. Fluid-based adhesion in insects—principles and challenges. Soft Matter 2011;7:11047–53.
[3] Dirks JH, Clemente CJ, Federle W. Insect tricks: two-phasic foot pad secretion prevents slipping. J R Soc Interface 2010;7:587–93.
[4] Clemente CJ, Dirks JH, Barbero DR, Steiner U, Federle W. Friction ridges in cockroach climbing pads: anisotropy of shear stress measured on transparent, microstructured substrates. J Comp Physiol A 2009;195:805–14.
[5] Kendall MD. The anatomy of the tarsi of *Schistocerca gregaria* Forskal. Z Zellforsch Mikrosk Anat 1970;109:112–37.
[6] Roth LM, Willis ER. Tarsal structure and climbing ability of cockroaches. J Exp Zoolog 1952;119:483–517.
[7] Scholz I, Baumgartner W, Federle W. Micromechanics of smooth adhesive organs in stick insects: pads are mechanically anisotropic and softer towards the adhesive surface. J Comp Physiol A 2008;194:373–84.
[8] Slifer EH. Vulnerable areas on the surface of the tarsus and pretarsus of the grasshopper (Acrididae, Orthoptera) with special reference to the arolium. Ann Entomol Soc Am 1950;43:173–88.
[9] Beutel RG, Gorb SN. Ultrastructure of attachment specializations of hexapods, (Arthropoda): evolutionary patterns inferred from a revised ordinal phylogeny. J Zoolog Syst Evol Res 2001;39:177–207.
[10] Gorb S, Jiao Y, Scherge M. Ultrastructural architecture and mechanical properties of attachment pads in *Tettigonia viridissima* (Orthoptera Tettigoniidae). J Comp Physiol A 2000;186:821–31.
[11] Gorb SN, Scherge M. Biological microtribology: anisotropy in frictional forces of Orthopteran attachment pads reflects the ultrastructure of a highly deformable material. Proc R Soc Lond B 2000;267:1239–44.
[12] Autumn K, Dittmore A, Santos D, Spenko M, Cutkosky M. Frictional adhesion: a new angle on gecko attachment. J Exp Biol 2006;209:3569–79.
[13] Federle W, Brainerd EL, McMahon TA, Hölldobler B. Biomechanics of the movable pretarsal adhesive organ in ants and bees. Proc Natl Acad Sci USA 2001;98:6215–20.
[14] Endlein T, Federle W. Ants can't be knocked off: a 'preflex' as an extremely rapid attachment reaction. Comp Biochem Phys A 2009;153:S138.
[15] Federle W, Endlein T. Locomotion and adhesion: dynamic control of adhesive surface contact in ants. Arthropod Struct Dev 2004;33:67–75.
[16] Höltje M, Hustert R. Rapid mechano-sensory pathways code leg impact and elicit very rapid reflexes in insects. J Exp Biol 2003;206:2715–24.
[17] Wilson DM. Proprioceptive leg reflexes in cockroaches. J Exp Biol 1965;43:397–409.
[18] Andersen SO, Weis-Fogh I. Resilin: a rubber-like protein in arthropodal cuticle. Adv Insect Physiol 1964;2:1–65.
[19] Burrows M, Shaw SR, Sutton GP. Resilin and chitinous cuticle form a composite structure for energy storage in jumping by froghopper insects. BMC Biol 2008;6:41.
[20] Fahle M. Human pattern recognition: parallel processing and perceptual learning. Perception 1994;23:411–27.
[21] Sutherland NS. Outlines of a theory of visual pattern recognition in animals and man. Proc R Soc Lond B 1968;171:297–317.
[22] Abramoff MD, Magelhaes PJ, Ram SJ. Image processing with ImageJ. Biophotonics Int 2004;11:36–42.
[23] Beauchemin SS, Barron JL. The computation of optical flow. ACM Comput Surv 1995;27:434–66.
[24] Federle W, Baumgartner W, Hölldobler B. Biomechanics of an adhesive pads: frictional forces are rate- and temperature-dependent. J Exp Biol 2004;207:67–74.
[25] Drechsler P, Federle W. Biomechanics of smooth adhesive pads in insects: influence of tarsal secretion on attachment performance. J Comp Physiol A 2006;192:1213–22.
[26] Neville AC. Biology of the arthropod cuticle. Berlin: Springer Verlag; 1975.
[27] Evans KE. Tensile network microstructures exhibiting negative Poisson's retios. J Phys D 1989;22:1870–6.
[28] Burke M. A stretch of the imagination. New Scientist 1997;154:36–9.
[29] Lakes RS. Foam structures with a negative Poisson's ratio. Science 1987;235:1038–40.
[30] Kaelble DH. Theory and analysis of peel adhesion: bond stresses and distributions. J Rheol 1960;4:45–73.